



Published in final edited form as:

J Child Neurol. 2015 September ; 30(10): 1343–1348. doi:10.1177/0883073814562252.

Early onset Aicardi Goutières syndrome: MRI pattern Recognition

Adeline Vanderver^{1,2}, Morgan Prust³, Nadja Kadom⁴, Scott Demarest², Yanick J Crow^{5,6}, Guy Helman², Simona Orcesi⁷, Roberta La Piana⁸, Carla Uggetti⁹, Jichuan Wang¹⁰, Heather Gordisch-Dressman¹⁰, Marjo S van der Knaap¹¹, and John H Livingston¹²

¹Center for Genetic Medicine Research, Children's National Health System Washington, DC, USA ²Department of Neurology, Children's National Health System, Washington, DC, USA ³Harvard Medical School, Harvard University, Boston, MA, USA ⁴Department of Radiology, Children's National Health System, Washington, DC, USA ⁵Manchester Academic Health Science Centre, University of Manchester, Genetic Medicine, Manchester, UK ⁶Department of Genetics, INSERM U781, Université Paris Descartes- Sorbonne Paris Cité, Institut Imagine, Hôpital Necker Enfants Malades (AP-HP), Paris 75015, France ⁷Child Neurology and Psychiatry Unit, C. Mondino National Neurological Institute, Pavia, Italy ⁸Department of Neuroradiology, Montreal Neurological Institute and Hospital, McGill University, Montreal, Quebec, Canada ⁹Unit of Neuroradiology, Department of Radiology, San Carlo Borromeo Hospital, Milano, Italy ¹⁰Department of Biostatistics, Children's National Health System, Washington, DC, USA ¹¹Department of Child Neurology, VU University Medical Center, Amsterdam, The Netherlands ¹²Department of Paediatric Neurology, Leeds Teaching Hospitals NHS Trust, Leeds, UK

Abstract

Aicardi Goutières syndrome (AGS) is an inherited leukodystrophy with calcifying microangiopathy and abnormal central nervous system myelination. As fewer diagnostic CT scans are being performed due to increased availability of MR imaging, there is a potential for missed diagnoses on the basis of calcifications. We review a series of patients with MRIs selected from IRB-approved leukodystrophy biorepositories to identify MRI patterns for recognition of early-onset AGS and scored for a panel of radiologic predictors. Each individual predictor was tested against disease status using exact logistic regression. Features for pattern recognition of AGS are temporal lobe swelling followed by atrophy with temporal horn dilatation, early global cerebral atrophy and visible calcifications, as evidenced by 94.44% of cases of AGS correctly classified with a sensitivity of 90.9% and specificity of 96.9%. We identify a panel of MRI features predictive of AGS in young patients that would differentiate it from other leukoencephalopathies.

Contact information: Adeline Vanderver, MD, Department of Neurology, Children's National Health System 111 Michigan Avenue, NW, Washington, DC 20010, Tel. 202 476 6230, Fax. 202 476 5226, avanderv@childrensnational.org.

Author Contributions: AV, YC, JL and MSK managed the project.

NK, RLP, CU, SD, SM, MSK, JL, YC, and AV performed MRI examination. HGD and JW designed the statistical analyses. AV, and HGD performed the data analyses. MP, SD, GH, YC, JL, MSK, and AV wrote the paper.

Disclosures: Otherwise, the authors report no conflicts of interest.

Keywords

Pediatric Neuroradiology; Leukodystrophies; Aicardi Goutières syndrome

Introduction

Aicardi Goutières syndrome (AGS) is an inherited leukoencephalopathy caused by mutations in *TREX1*,¹ *SAMHD1*,² *RNASEH2A*, *RNASEH2B* and *RNASEH2C*,³ *ADARI*,⁴ and *IFIH1*.⁵ These genes, when mutated, are believed to cause an accumulation of immune stimulatory nucleic acids and activation of innate cellular immunity, resulting in the characteristic phenotype of cerebral spinal fluid (CSF) pleocytosis, increased CSF alpha interferon and a calcifying microangiopathy with abnormal central nervous system white matter.⁶ Classically, this diagnosis is suspected when typical calcifications are identified on CT imaging in the appropriate clinical context.

Due to the increased availability of MR imaging and to concerns with exposure to radiation, fewer CT scans are now performed as part of a diagnostic evaluation. This may result in missed opportunities to diagnose AGS, unless characteristic MRI patterns are identified that permit suspicion of the disorder and appropriate diagnostic testing. In addition, patients without calcifications at disease onset have been identified⁷⁻¹⁰ so that a lack of cerebral calcifications cannot be considered an exclusionary criterion.^{7, 11, 12}

For these reasons, it is important to explore the diagnostic utility of MRI in AGS, in particular in early onset cases in the first year of life. In addition to intracranial calcifications, AGS has been associated with abnormal cerebral white matter and cerebral atrophy.¹¹⁻¹⁶ White matter abnormalities may be either diffuse or with an anterior-posterior gradient including a swollen appearance of anterior frontal and anterior temporal gyri.^{7, 17} Younger patients and patients with the antero-posterior gradient were also likely to have fronto-temporal cysts as additional features.⁷ Finally, early onset atrophy is also a prominent finding in a majority of AGS patients,⁷ and it may be progressive, involving the entire cerebral hemispheres,⁷ and brainstem,¹⁸ with relative cerebellar sparing.⁷

Differential diagnosis of the combination of calcification, atrophy and swollen frontal or temporal white matter with or without cysts is particularly challenging in the first two years of life, as these may be seen in a number of early-onset disorders of the white matter (Figure 1). These include acquired white matter diseases, such as congenital infections (e.g. Cytomegalovirus or Rubella). Additionally, certain inherited disorders of the white matter, or leukodystrophies can demonstrate overlapping radiologic findings. These include: Alexander disease (AxD) (presence of cysts and frontal predominance), Megalencephalic Leukoencephalopathy with subcortical cysts (MLC) (prominent temporal involvement and cysts), Vanishing white matter disease (VWM) (rarefaction of white matter, temporal cysts in severe variants), RNaseT2 related disease (temporal lobe cysts), Rubella, mitochondrial leukoencephalopathies (temporal lobe involvement), various types of congenital muscular dystrophies (FCMD, Walker Warburg syndrome, MDC1D) (temporal lobe involvement), and Leukoencephalopathy with Calcifications and Cysts (LCC) (cysts and calcifications).

We sought to identify a panel of MRI features predictive of AGS in very young patients that would differentiate it from other white matter diseases that present with similar radiologic features, and permit the clinician to order appropriate diagnostic testing.

Methods

Standard Protocol Approvals, Registrations, and Patient Consents

MRI images of patients with mutation proven AGS (n=23, including AGS1=14, AGS2=3, AGS3=3, AGS5=3), infantile AxD (n=9), MLC (n=5), congenital CMV (n=4), LCC (n=3) and VWM (n=9) were reviewed according to a standard protocol. Imaging studies from patients with proven leukodystrophies with infantile onset were selected. Age of first MRI and basic clinical information was recorded. All patients were selected from as part of an IRB-approved biorepository of leukodystrophy subjects collected from clinical centers with expertise in these disorders. Informed consent was obtained from all the patients evaluated at Children's National Health System and the University of Manchester.

Radiologic Criteria

All MRIs were scored for a series of radiologic predictors including: cerebral, cerebellar and brainstem atrophy; location of white matter abnormalities; presence within abnormal white matter of regions of hypointense T₂ signal or hyperintense T₁ signal suggesting areas of more normal myelin development or mineralization; more hyperintense T₂ signal in an irregular fashion in subcortical regions; evidence of white matter rarefaction on FLAIR imaging, visibility of calcifications on standard T₁ and T₂ imaging (as confirmed with correlation by CT scan review) on MRI; basal ganglia signal abnormalities and atrophy, cystic changes within brain parenchyma; and the finding of swelling or focal atrophy of areas including the frontal or temporal lobes (Figure 2). MRIs were scored by a pediatric neuroradiologist (NK) who was blinded to the patient's diagnosis.

Statistical Analysis

Each individual predictor was tested against disease status (AGS vs. non-AGS) using exact logistic regression. All predictors with a p-value less than 0.05 were compared pair-wise to determine which predictors exhibit co-linearity. Unique predictors having a significant relationship with disease status were included in a stepwise logistic regression model (probability criteria for exclusion/inclusion set to 0.2). All predictors entered into the model had equal chance of retention/exclusion at each step. The final model was developed by combining results from the stepwise process and iteratively including/excluding predictors felt to be most clinically relevant while accessing model fit via the Bayesian information criterion. Odds ratios, p-values and 95% confidence intervals are reported for those predictors surviving the selection process. A classification table was prepared for this final model.

Results

All proposed predictors appeared individually statistically predictive of AGS, with the exception of a thin corpus callosum, signal abnormalities in the basal ganglia and cerebellar

white matter, and swollen appearing white matter in the parietal regions. Exact logistic regression analysis of each variable against diagnosis of AGS identified 13 variables with p values <0.05 (Table 1). However, multiple-variable logistic regression analysis identified a combined model that included only a few of these features (Table 2). This correctly identified 94.44% of cases of AGS present in this sample (Sensitivity 90.91%, Specificity 96.88%, Positive Predictive value 95.24%, Negative Predictive value 93.94%). These results were used in preparation of a diagnostic algorithm based on the proposed predictors of AGS based on the retained clinical predictors (Figure 3).

Patient's ages were a mean 1.2 years, median 0.7 year; while controls were a mean 3.4 years, median 2.2 years. All patients where data was available in both the AGS and control groups were developmentally delayed early in their clinical presentations: 23/23 (100%) of AGS cases and 23/23 (100%) of control cases. There was a higher frequency of gastrostomy tube (G-Tube) feeding dependence in the AGS population (11/16 where data was available or 69%) versus the control population (5/19 where data was available or 26%) (supplemental data Table 1). Similarly, fewer of the AGS patients than controls were ambulatory or verbal, though this may be in part a reflection of their younger age. Exact logistic regression was used in this analysis due to small sample size.

Discussion

This approach develops an algorithm for early onset leukodystrophies, to aid in the analysis of MRIs felt to be possibly consistent with AGS. The combination of temporal lobe swelling or temporal horn dilation, with progressive atrophy, in particular of the frontal lobe, appears fairly specific of AGS. Also notable was the fact that when carefully sought, calcifications were often visible on standard T₁ and T₂ MRI images, and when identified were highly specific for AGS. Together, these features can help suggest a diagnosis of AGS, and can be used by the clinician to determine the need for a CT scan or specific MRI modalities to identify calcifications and may prompt molecular or biochemical testing.

It is important to note that this algorithm was developed from leukoencephalopathies with features that could be overlapping with AGS, such as a temporal or frontal predominance of leukoencephalopathy or presence of calcifications, and still needs to be validated in a larger cohort of unsolved leukodystrophies. Additionally, this model is developed from and for patients with early onset leukoencephalopathies and may not be pertinent in AGS patients with later age of onset.⁷

Additional limitations of the study included lack of perfect age matching of the samples. This is a reflection of the fact that these diseases have slightly different typical ages of onset, and therefore slightly different ages of available MRI studies. Also of note, a predominance of patients with AGS in this study had mutations in *TREX1*, and patients with mutations in the other genes were underrepresented. This is in part determined by the fact that cases were selected based on early age at onset, and first imaging. Patients with *TREX1* mutations are more likely to have an earlier onset and we cannot definitely exclude that the observed results - i.e. the specificity of temporal pole swelling and cystic degeneration - reflect the peculiar distribution of the mutated genes in our sample.

Finally, as is often the case in rare disease research, our small sample size limited the range of feasible statistical analyses. In order to decrease the risk of statistical over-fitting, where the developed model is only applicable to the sample at hand and not generalizable to the population, we took an iterative approach where we evaluated each predictor and the effect of a combination of predictors to arrive at a model that balances fit to the data with generalizability. Despite the high quality of fit, our results were based on only 23 AGS patients and 30 non-AGS control subjects as evidenced by the very wide confidence intervals. As the number of leukoencephalopathies with similar MRI features are discovered and additional patients are found and included in the analysis, the results presented here may change.

Additionally, although a number of other disorders may have overlapping radiologic features with AGS, such as temporal or frontal lobe predominance, calcifications, and cysts, these typically have other characteristics that may permit pattern recognition. These non AGS relevant MRI characteristics were not scored, as our small sample size precluded the statistical analysis of a larger set of variables. For example, these include: in AxD findings of basal ganglia and brainstem findings, as well as the extensive contrast enhancement; in MLC persistently swollen gyri and late atrophy with sometimes extensive cysts; in VWM disease significant rarefaction of affected white matter; and in LCC, the globular nature of calcifications in large aggregates and the large intra-parenchymal cysts.

The proposed algorithm therefore does not take into consideration the full complexity of recognizing a likely diagnosis in an individual MRI. The entire constellation of clinical and radiologic features should be appreciated in each patient during diagnostic work-up. However, features of temporal lobe swelling followed by atrophy with temporal horn dilatation, early global cerebral atrophy and visible calcifications on MRI appears to be a promising group of features for pattern recognition on MRI in young patients with AGS. These features may help a clinician recognize AGS in an era where CT scans are less often performed, and there is a greater potential for missing the pathognomonic calcifications seen in this disorder.

These diagnostic imaging markers present a phenotype that is useful in evaluating MRI features in the diagnosis of early AGS versus other early-onset leukodystrophies, further validating previous descriptions of this early onset AGS phenotype.^{7, 19}

Supplementary Material

Refer to Web version on PubMed Central for supplementary material.

Acknowledgements

the authors would like to thank the families of the patients included in this study, as well as the Myelin Disorders Bioregistry Project. This study was partially funded by the European Union's Seventh Framework Programme (FP7/2007-2013) under grant agreement 241779, a European Research Council (GA 309449) grant to YJC. The participation of Morgan Prust and Guy Helman was supported by the Delman fund and the Neurogenetics Program at Children's National Health System. We would also like to thank Luca Ramenghi for images of a patient with congenital rubella and Dr. Raphael Schiffman for contributing patients.

AV provides unpaid consulting to StemCells Inc. Her involvement was supported by a K08 from NINDS.

References

1. Crow YJ, Hayward BE, Parmar R, et al. Mutations in the gene encoding the 3'-5' DNA exonuclease TREX1 cause Aicardi-Goutieres syndrome at the AGS1 locus. *Nat Genet.* 2006; 38(8):917–920. [PubMed: 16845398]
2. Rice GI, Bond J, Asipu A, et al. Mutations involved in Aicardi-Goutieres syndrome implicate SAMHD1 as regulator of the innate immune response. *Nat Genet.* 2009
3. Crow YJ, Leitch A, Hayward BE, et al. Mutations in genes encoding ribonuclease H2 subunits cause Aicardi-Goutieres syndrome and mimic congenital viral brain infection. *Nat Genet.* 2006; 38(8):910–916. [PubMed: 16845400]
4. Rice GI, Kasher PR, Forte GM, et al. Mutations in ADAR1 cause Aicardi-Goutieres syndrome associated with a type I interferon signature. *Nat Genet.* 2012; 44(11):1243–1248. [PubMed: 23001123]
5. Rice GI, Del Toro Duany Y, Jenkinson EM, et al. Gain-of-function mutations in IFIH1 cause a spectrum of human disease phenotypes associated with upregulated type I interferon signaling. *Nat Genet.* 2014
6. Goutieres F, Aicardi J. Acute neurological dysfunction associated with destructive lesions of the basal ganglia in children. *Ann Neurol.* 1982; 12(4):328–332. [PubMed: 7149658]
7. Uggetti C, La Piana R, Orcesi S, Egitto MG, Crow YJ, Fazzi E. Aicardi-Goutieres syndrome: neuroradiologic findings and follow-up. *AJNR American journal of neuroradiology.* 2009; 30(10):1971–1976. [PubMed: 19628626]
8. Aicardi J, G F. A progressive familial encephalopathy in infancy with calcifications of the basal ganglia and chronic cerebrospinal fluid lymphocytosis. *Ann Neurol.* 1984; 15(1):49–54. [PubMed: 6712192]
9. D'Arrigo S, Riva D, Bulgheroni S, et al. Aicardi-Goutières syndrome: description of a late onset case. *Developmental Medicine & Child Neurology.* 2008; 50(8):631–634. [PubMed: 18754903]
10. Goutieres F, Aicardi J, Barth PG, Lebon P. Aicardi-Goutieres syndrome: an update and results of interferon-alpha studies. *Ann Neurol.* 1998; 44(6):900–907. [PubMed: 9851434]
11. Crow YJ, Livingston JH. Aicardi-Goutieres syndrome: an important Mendelian mimic of congenital infection. *Dev Med Child Neurol.* 2008; 50(6):410–416. [PubMed: 18422679]
12. Orcesi S, La Piana R, Fazzi E. Aicardi-Goutieres syndrome. *Br Med Bull.* 2009; 89:183–201. [PubMed: 19129251]
13. Goutieres F. Aicardi-Goutieres syndrome. *Brain Dev.* 2005; 27(3):201–206. [PubMed: 15737701]
14. Lanzi G, Fazzi E, D'Arrigo S. Aicardi-Goutieres syndrome: a description of 21 new cases and a comparison with the literature. *Eur J Paediatr Neurol.* 2002; 6(Suppl A):A9–A22. discussion A3-5, A77-86. [PubMed: 12365365]
15. Lanzi G, Fazzi E, D'Arrigo S, et al. The natural history of Aicardi-Goutieres syndrome: follow-up of 11 Italian patients. *Neurology.* 2005; 64(9):1621–1624. [PubMed: 15883328]
16. Ostergaard JR, Christensen T. Aicardi-Goutieres syndrome: neuroradiological findings after nine years of follow-up. *Eur J Paediatr Neurol.* 2004; 8(5):243–246. [PubMed: 15341906]
17. Van der Knaap, M. *Magnetic Resonance of Myelination and Myelin Disorders.* third ed. Berlin: Springer-Verlag; 2005. p. 284-342.
18. Crow YJ, Massey RF, Innes JR, et al. Congenital glaucoma and brain stem atrophy as features of Aicardi-Goutières syndrome. *American Journal of Medical Genetics Part A.* 2004; 129A(3):303–307. [PubMed: 15326633]
19. van der Knaap, M.; Valk, J. *Magnetic Resonance of Myelination and Myelin Disorders.* 3. ed. Berlin, Germany: Springer; 2005.

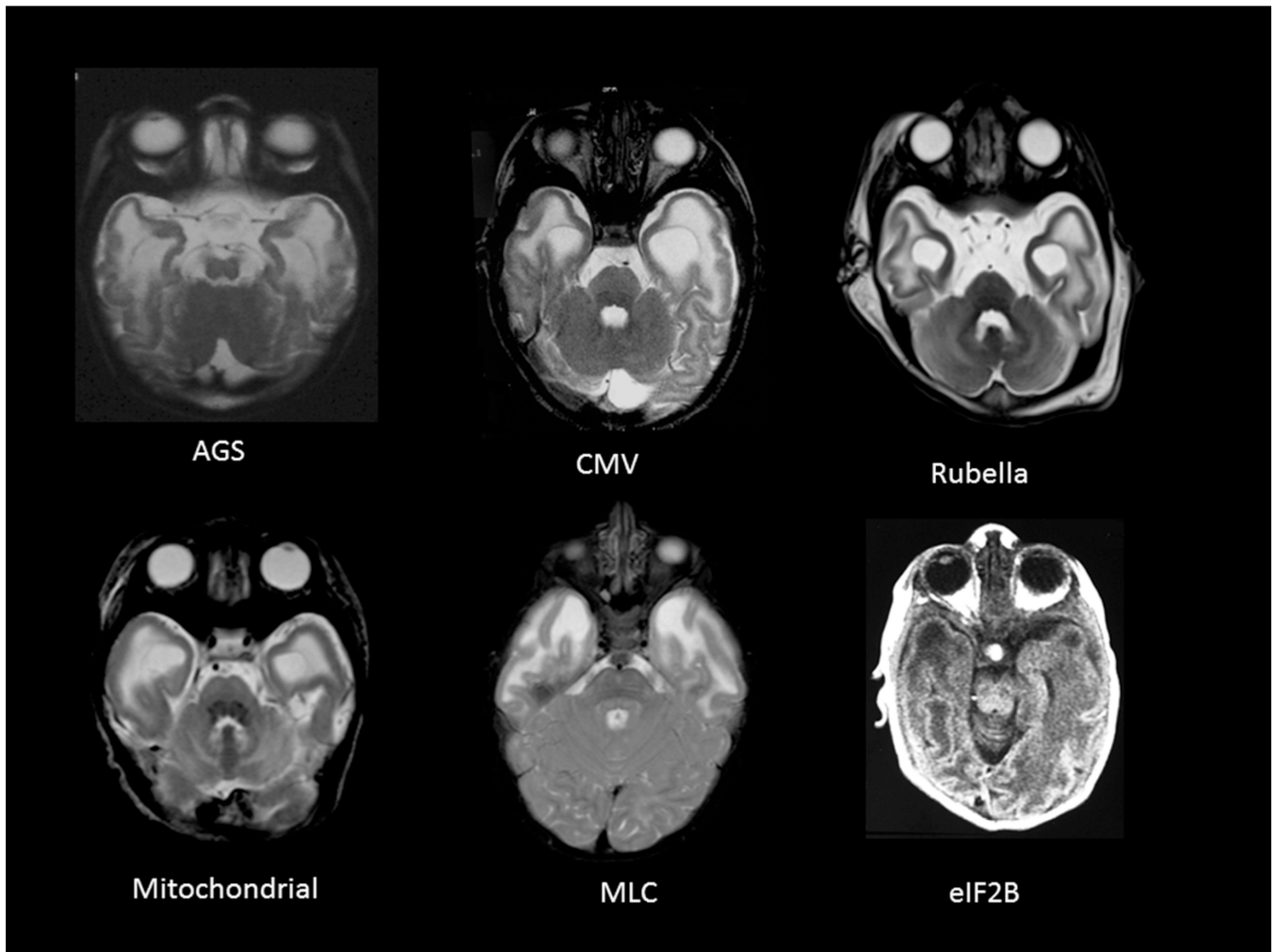


Figure 1. Swollen temporal lobes on MRI

may have many causes including a few depicted here: Aicardi Goutières syndrome (AGS), Congenital infection with Cytomegalovirus (CMV) or Rubella, mitochondrial leukoencephalopathies, Megalencephalic leukodystrophy with cysts – (MLC) and antenatal onset vanishing white matter with *eIF2B* mutations. In addition, reported cases include, cystic leukoencephalopathy without megalencephaly due to *RNASET2* mutations and various types of congenital muscular dystrophies (FCMD, Walker Warburg syndrome, MDC1D).

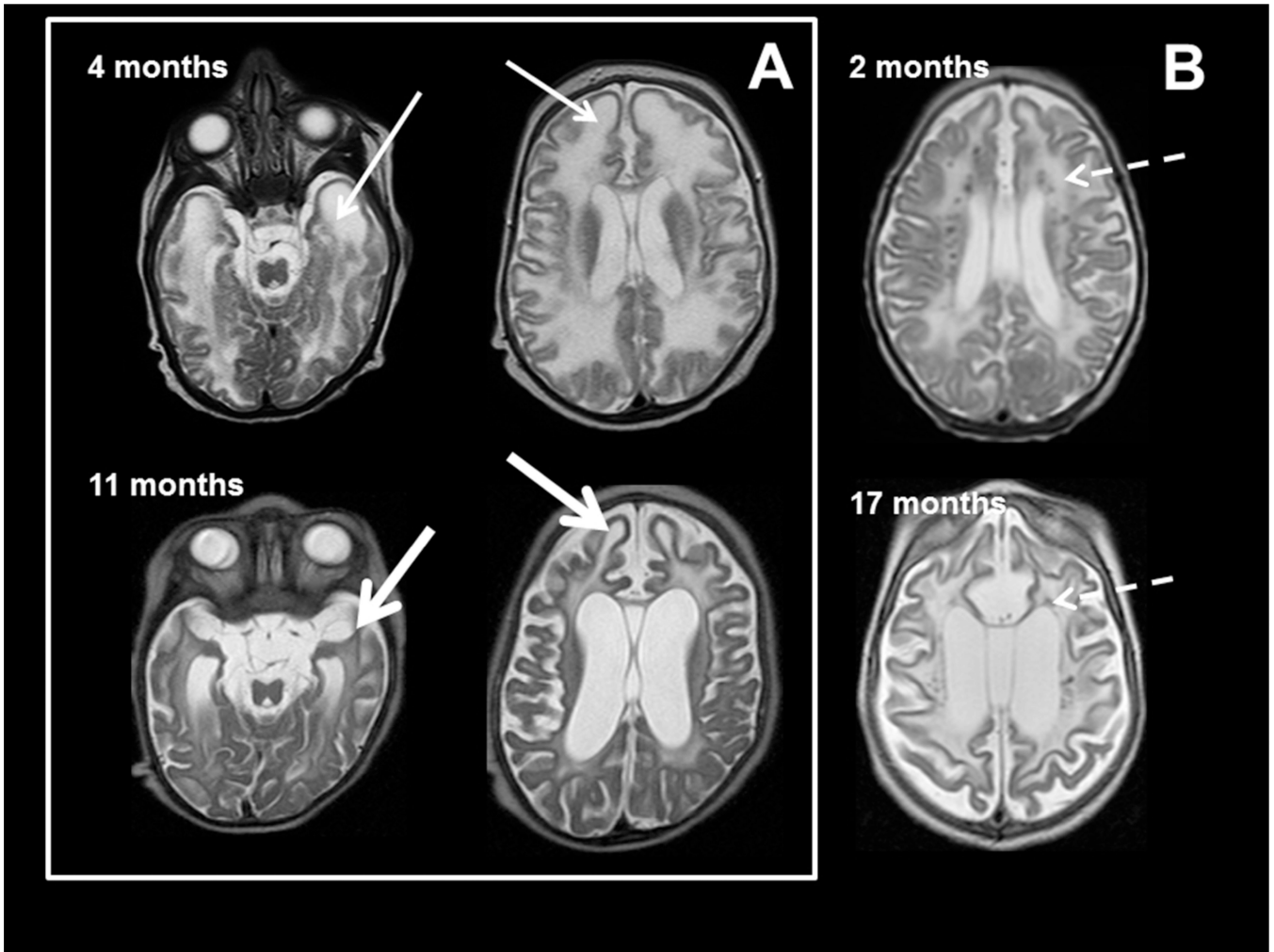


Figure 2. MRI characteristics in AGS

MR imaging obtained in two patients with AGS at age 4 months (upper row) and 11 months (lower row) of age in box A and the second patient with images at 2 and 17 months (B). The images demonstrate early frontal and temporal lobe swelling (thin white arrow) that gives way to severe frontal and temporal lobe atrophy (thick white arrows), as well as the prominent global atrophy. Note also the T₂ dark signal abnormalities presumed to be calcifications present at 2 months and present at 17 months in the second patient (dashed arrows).

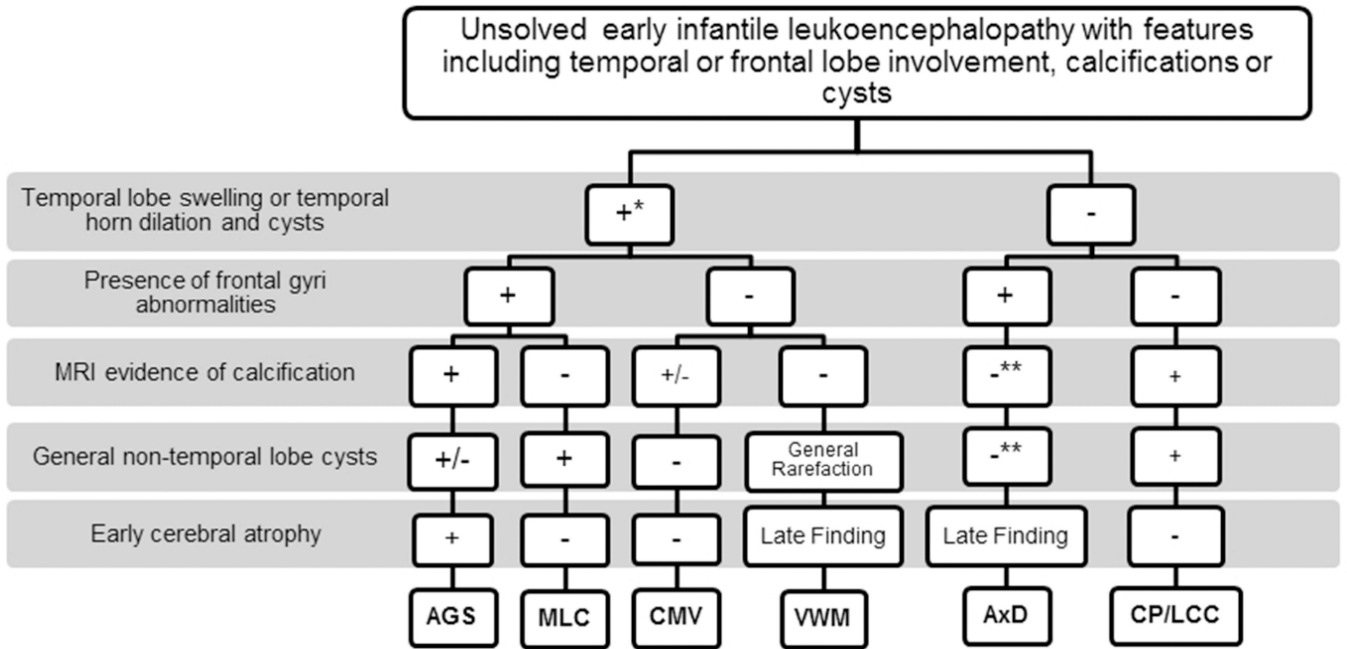


Figure 3. MRI characteristics of unsolved early infantile leukoencephalopathy

MRI analyses were used to identify a possible descriptive algorithm of features on MRI consistent with the diagnosis of Aicardi Goutières syndrome (AGS). Features of radiologic findings from Megalencephalic Leukoencephalopathy with subcortical cysts (MLC), Cytomegalovirus (CMV), Vanishing white matter disease (VWM), Alexander disease (AxD) and Coats Plus disease/Leukoencephalopathy with Calcifications and Cysts (CP/LCC) are depicted. Note the features of temporal lobe swelling followed by atrophy with temporal horn dilatation, early global cerebral atrophy and visible calcifications on MRI in young patients with AGS. This appears to be a promising group of features for pattern recognition on MRI.

*Temporal lobe swelling occurs in early infantile cases of VWM, while it is not an MRI feature found in late-onset VWM patients. In addition, early infantile cases frequently have anterior temporal cysts.

**Indicates a generally rare feature but exceptions have been found.

Table 1

Testing each predictor against disease status

Predictor	OR	95% CI	P-value
Cerebral atrophy	25.65	6.08 – 108.24	<0.0001
Brain stem atrophy or hypoplasia	25.67	4.96 – 132.94	<0.0001
Cerebral WM loss/ventricular dilation	36.67	4.37 – 307.92	0.001
Irregular high signal T ₂ in cerebral subcortical region	13.56	1.53– 120.03	0.019
Anterior >Posterior gradient on T ₁ or T ₂	7.92	2.29 – 27.40	0.001
Low signal T ₂ in WM	0.25	0.08 – 0.78	0.019
Calcification on MR	19.44	4.91 – 76.93	<0.0001
Cerebellar WM abnormal	1.66	0.56 – 4.96	0.364
Basal ganglia signal abnormal	1.47	0.50 – 4.33	0.481
Basal ganglia atrophy	6.42	1.70 – 24.24	0.006
Corpus callosum thin	5.50	0.61 – 49.37	0.128
Cysts, non temporal	3.27	1.01 – 10.56	0.047
Temporal horn dilation	14.73	3.88 – 55.99	<0.0001
Frontal gyri swelling	2.08	0.70 – 6.23	0.190
Frontal atrophy	11.54	2.21 – 60.19	0.004
Swollen temporal pole	5.26	1.56 – 17.76	0.007
Temporal atrophy	33.82	3.93 – 291.15	0.001
Mid parietal swollen gyri	1.93	0.61 – 6.14	0.266

* WM, white matter

Table 2

Best fit model

Predictor	OR	SE	OR 95% CI	Coefficient	p-value
Swollen temporal pole	25.25	37.70	1.35 – 471.09	3.229	0.032
Temporal horn dilation	40.35	58.79	2.32 – 701.66	3.698	0.011
Calcification visible on MRI	14.99	19.71	1.14 – 197.23	2.707	0.039
Cerebral atrophy	86.17	138.51	3.69 – 2012.04	4.456	0.006